ISSN 1028-334X, Doklady Earth Sciences, 2018, Vol. 481, Part 1, pp. 958–962. © Pleiades Publishing, Ltd., 2018.
Original Russian Text © G.M. Shved, G.S. Golitsyn, S.I. Ermolenko, A.E. Kukushkina, 2018, published in Doklady Akademii Nauk, 2018, Vol. 481, No. 3.

GEOPHYSICS

Relationship of the Long-Period Free Oscillations of the Earth with Atmospheric Processes

G. M. Shved[a], *, Academician G. S. Golitsyn[b], S. I. Ermolenko[a], and A. E. Kukushkina[a]

Received April 4, 2018

Abstract—Based on the five-year record of the superconducting gravimeter in Strasburg (48.6° N, 7.7° E), the correlation is calculated between the long-period free oscillations of the Earth and the Arctic Oscillation and Antarctic Oscillation indices of atmospheric circulation. The statistically significant correlations for the ${}_0S_2$, ${}_0T_2$, ${}_0T_3$, and ${}_0S_5$ oscillations show that their excitation on seismically quiet days is at least partly due to dynamic processes in the atmosphere.

DOI: 10.1134/S1028334X18070292

INTRODUCTION

The subject of this article is the relationship of the Earth's free oscillations (EFOs) with dynamic processes in the atmosphere.

In the late 1990s, two groups of seismologists simultaneously reported the evidence of an incessant background of short-period spheroidal EFOs from ${}_0S_{12}$ to ${}_0S_{65}$ (periods of ~2–8 min, frequencies of ~2–7 mHz) on seismically quiet days [1, 2]. An attempt to associate the background with the cumulative effect of small earthquakes was unsuccessful [1, 3]. However, studies revealed a seasonal variation in the intensity of the background with two maxima: in winter and in summer (see, e.g., [4]). This variation suggested that the primary source of background EFOs was atmospheric processes. Subsequent studies [5, 6] located the predominant sources of background EFOs. In the Northern Hemisphere, EFOs originate mainly in the northern Pacific Ocean during winter in the Northern Hemisphere; in the Southern Hemisphere, they form in a bracelike band from the eastern to western Pacific Ocean through Southern ocean (to the south of the Atlantic and Indian Oceans), also during winter in the Southern Hemisphere.

Speaking about long-period EFOs, the excitation of the one with the longest period—the spheroidal 54-min ${}_0S_2$ oscillation—on seismically quiet days was reported even earlier [7]. Subsequently, the presence of an incessant background formed by long-period spheroidal EFOs was confirmed in [1]. However, no hypotheses were proposed to explain this phenomenon. The first attempt at relating the existence of background ${}_0S_2$ EFOs with atmospheric processes was made in [8] from the one-year record of an STS-2 seismometer at Collm (51.3° N, 13.0° E). The intensity of the power spectrum in the frequency range of the ${}_0S_2$ multiplet was compared with the Arctic Oscillation (AO) index, which characterizes the dynamic activity of the atmosphere at the middle and high latitudes of the Northern Hemisphere. A statistically significant, albeit small (with a correlation coefficient of ~0.1–0.2), correlation was obtained between the AO index and ${}_0S_2$ EFO.

While retaining the methodology of [8], we extended the analysis of atmospheric effects on long-period EFOs to a frequency of 900 μHz (period of ~18 min); used five-year series of seismic measurements made with an instrument of a different type and at a different locality; and incorporated the Antarctic Oscillation (AAO) index, which shows the atmospheric dynamics in the Southern Hemisphere, into the analysis.

INPUT DATA

We used measurement data from the superconducting gravimeter in Strasburg, France (48.6° N, 7.7° E), with a sampling interval of 1 min, which are available at http://isdc.gfz-potsdam.de/. To investigate the relationship of the EFOs with atmospheric processes, we chose a series of continuous measurements from November 1, 2011, to October 31, 2016. Furthermore, we added measurements obtained in the time vicinity of strong earthquakes: in Peru on June 23, 2001 (with a magnitude of $M = 8.4$), and on the Island of Sumatra on December 26, 2004 ($M = 9.1$). For the above-mentioned five-year

[a] *St. Petersburg State University, St. Petersburg, 199034 Russia*
[b] *Obukhov Institute of Atmospheric Physics, Russian Academy of Sciences, Moscow, 119017 Russia*
**e-mail: g.shved@spbu.ru*

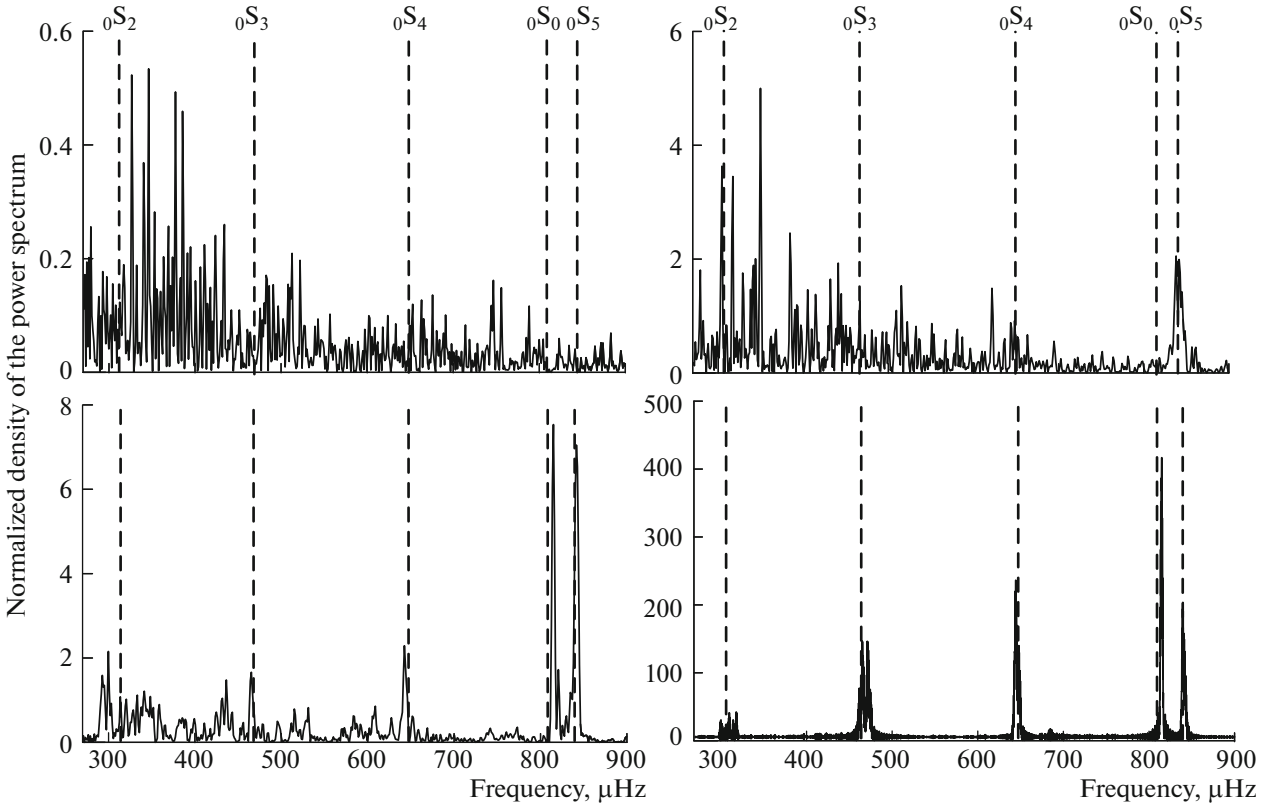

Fig. 1. Spectral power density before the earthquake (top) and after it (bottom) for the earthquakes in Peru (left) and on the Island of Sumatra (right). The vertical dashed lines correspond to the theoretical central frequencies of the Earth's free oscillations. Since the figure shows the normalized spectra, the spectral peaks in the background noise after the earthquake due to the excitation of the EFOs are manifested poorly.

period, we used daily AO and AAO indices from the website ftp://ftp.cpc.ncep.noaa.gov/cwlinks/.

RESEARCH METHODOLOGY

To rule out the effect on the EFOs of lower frequency oscillations detected by the gravimeter, spectral analysis was preceded by a Lanczos filtering of the measurement series with a cutoff frequency of 270 μHz (period of ~62 min).

Since the EFOs, like atmospheric normal modes (ANMs), are unsteady waves, we applied the spectral analysis methodology developed for ANMs in a period range of hours [9]. Following this methodology, we split the five-year measurement series into five-day segments sliding along the series with a one-day step. We conducted spectral analysis of these segments, with a total number of $N = 1821$, by the Lomb–Scargle method, thus ensuring a spectral resolution of 2.32 μHz. The spectra were presented with a frequency step of 1.16 μHz.

We used N values of the spectral intensity for each frequency to calculate the correlation coefficient r between this intensity and the AO and AAO indices, whereby we associated the spectrum of each five-day measurement series with the index values averaged over the same five days. The statistical significance of the resulting r coefficients was estimated by Student's t-tests.

RESULTS AND DISCUSSION

Long-period EFOs are excited by strong earthquakes. Relevant examples are given in [10, 11] for the earthquake of 2001 in Peru from superconducting gravimeter measurements and in [11–13] for the earthquake of 2004 on the Island of Sumatra from measurements made with various seismic instruments. Figure 1 allows a comparison of the spectra obtained from the five-day measurement series before and after the earthquakes. Apart from the well-known earthquake excitation of spheroidal fundamental modes, the figure shows that in the absence of strong earthquakes, there is background noise in which these EFOs manifest themselves from time to time, as is evident in the right panel of Fig. 1, which shows confident indications of the $_0S_5$ EFO as well as two peaks, which most likely represent the $_0S_2$ EFO.

The AO (AAO) indices of atmospheric circulation characterize the change in the longitude-averaged

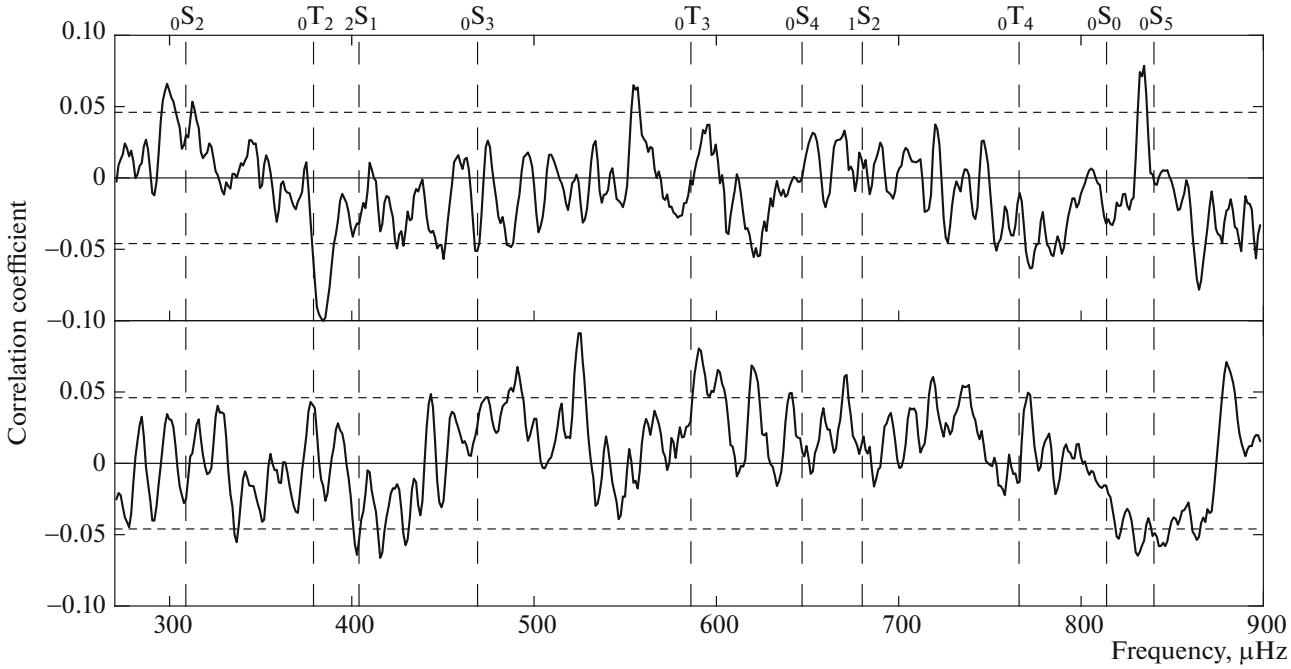

Fig. 2. Correlation coefficient r between the spectral intensity and the AO index (top) and AAO index (bottom). The values of $|r|$ beyond the limits indicated by the horizontal dashed line correspond to a confidence level above 95%. The vertical dashed lines correspond to the theoretical central frequencies of the Earth's free oscillations.

height z of the atmospheric pressure surface with p = 1000 (700) hPa in the Northern (Southern) Hemisphere with the transition from the middle to high latitudes. The AO index actually describes the change in the surface pressure of the atmosphere in the Northern Hemisphere. Since ground-based observation stations in the Southern Hemisphere are few in number, data on the atmospheric parameters in this hemisphere are obtained mainly by remote sensing methods from satellites. Therefore, the AAO index is calculated by necessity for a surface with p = 700 hPa: this index describes the change in atmospheric pressure at heights of about 3 km. Since the influence of atmospheric processes on geodynamic ones occurs at the lower boundary of the atmosphere, the AAO index is a less reliable indicator of atmospheric processes than the AO index.

The change in the height z of a specified isobaric surface along the meridian can conveniently be described by a gradient $\partial z/\partial y$, where y is the coordinate along the south–north direction. On average, the surface atmospheric pressure is observed to decrease from the middle latitudes poleward in both hemispheres. The AO and AAO indices are positive (negative) when they reflect a situation in which the absolute value of $|\partial z/\partial y|$ is greater (less) than the average value of $|\partial z/\partial y|$. Thus, an increase in the index corresponds to an increase in the pressure differential between the middle and high latitudes.

In the troposphere, the pressure and wind fields are related with each other with good accuracy by the geostrophic wind equation. According to this equation, the wind speed along the parallel (zonal wind) is

$$u = -\frac{g}{2\Omega\sin\varphi}\frac{\partial z}{\partial y}, \quad (1)$$

where g is the gravitational acceleration; Ω is the angular speed of rotation of the Earth; and φ is the latitude counted from the equator ($\varphi < 0$ in the Southern Hemisphere). Thus, an increase in the AO and AAO indices corresponds to an increase in the longitude-averaged zonal wind directed eastward at mid-latitudes. The stronger the zonal wind, the more likely instability of the atmospheric zonal flow, which leads to the appearance of extratropical cyclones. However, the cyclonic activity is accompanied by the appearance of strong perturbations in the pressure and wind fields near the surface in a wide range of spatial and temporal scales. Therefore, the AO and AAO indices can be considered as indicators of the dynamic activity of the atmosphere.

The frequency dependences of the correlation coefficient r after applying the moving average procedure over five frequencies (over an interval of 5.8 μHz) are presented in the range of 270–900 μHz in Fig. 2. Statistically significant correlation coefficients were obtained in the range $|r| = 0.05–0.10$ for the $_0S_2$, $_0T_2$, and $_0S_5$ EFOs (r reaches 0.14 for $_0S_5$) for the AO index and for the $_0T_3$ and $_0S_5$ EFOs for the AAO index.

For the $_0S_2$ EFOs we confirmed, although with lower values of r, the positive correlation previously

obtained in [8] of these oscillations with the AO index on seismically quiet days. The presence of a relationship between the ${}_0S_2$ EFOs and atmospheric processes is also confirmed by the two-hump contour of r in the frequency range of the ${}_0S_2$ multiplet. This shape of the contour stems from the fact that the relative intensity of the EFO components varies with latitude [12]. The detection of the ${}_0S_5$ EFO in the spectra on seismically quiet days (see also Fig. 1) indicates the higher probability that its excitation is related to atmospheric processes. However, for the correlations with the AO and AAO indices, the r coefficient at frequencies compatible with the ${}_0S_5$ EFO has different signs.

Gravimetric measurements after strong earthquakes also detect toroidal ${}_0T_2$, ${}_0T_3$, and ${}_0T_4$ EFOs [10, 14], the amplitude of which is, however, much less than that of the spheroidal EFOs. The appearance of gravimetrically detectable vertical motion at the frequencies of the toroidal EFOs is associated with the interaction of the spheroidal and toroidal EFOs due to the Coriolis force [14]. Noteworthy is the fact that the values of $|r|$ at the frequencies of the ${}_0T_2$ and ${}_0T_3$ EFOs in Fig. 2 are no less in order of magnitude than those of $|r|$ at the frequencies of the ${}_0S_2$ and ${}_0S_5$ EFOs, with the ${}_0T_2$ EFO demonstrating a negative correlation with the AO index.

The spectral analysis of the 1.5-year data from the superconducting gravimeter in Strasbourg revealed in the frequency range under consideration numerous high harmonics of the solar day, which are associated with solar thermal tides [15]. It is likely that some of the statistically significant extrema in the frequency dependence of r in Fig. 2 are due to these tides. Their detection indicates that the AO and AAO indices reflect the atmospheric processes that affect the generation of these tides. However, we cannot rule out that some of the statistically significant extrema are random.

The toroidal EFOs can be excited by variations in the near-surface wind on land and/or by those in the velocity of bottom currents in the oceans and seas due to the friction of air and/or water against the surface. As for the spheroidal EFOs, they can also be excited by variations in atmospheric and/or water pressure, leading to the corresponding vertical motion of the lithosphere. As for the specific mechanisms underlying the generation of the EFOs by atmospheric processes, for now one can only construct hypotheses. For example, it was suggested in [5] that the EFOs in the period range of minutes (discussed in the Introduction) are due to strong winds leading to strong oceanic surface waves: the EFOs are excited by internal gravity waves in the water, which originate from the surface waves and affect the seabed.

The negative correlation between the ${}_0T_2$ EFO and the AO index and between the ${}_0S_5$ EFO and the AAO index may reflect the existing complex pattern of interaction of atmospheric processes: the strengthening of some processes may lead to the weakening of others, including those responsible for the excitation of the EFOs. The negative correlation between the ${}_0T_2$ EFO and the AO index may also be explained by the weakening of the interaction between the ${}_0T_2$ EFO and spheroidal EFOs with the strengthening of the atmospheric processes that are described by the AO index. The fact that Fig. 2 shows no explicit signs of excitation of the ${}_0S_3$ and ${}_0S_4$ EFOs may be explained, at least in part, by the features of the observation site. Moreover, Fig. 2 shows no manifestations of the ${}_0S_0$ EFOs, which often prove to be the strongest after earthquakes (see Fig. 1), and the ${}_2S_1$ and ${}_1S_2$ EFOs. However, this is something to be expected because their excitation requires a source on the Earth, a circumstance that serves as indirect evidence of the reliability of our results.

It should be noted that the generation of seismic oscillations by atmospheric motions directly or indirectly through waves in water basins is a long-known phenomenon. Firstly, these are microseisms with periods from hundredths of a second to ~10 s, which are caused by wind gusts and sea waves breaking into the shore. Secondly, these are seismic oscillations recorded in the coastal zone, which are due to seiches, i.e., wind-caused standing waves in entirely and partly closed water-basins with periods from ~1 min to ~1 day.

CONCLUSIONS

It is shown, for the first time, that the excitation of the long-period ${}_0T_2$, ${}_0T_3$, and ${}_0S_5$ EFOs on seismically quiet days is at least partly due to dynamic processes in the atmosphere. The same conclusion is confirmed for the ${}_0S_2$ EFO.

ACKNOWLEDGMENTS

We thank T.B. Yanovskaya for the comments made after reading the manuscript, which allowed us to improve the presentation of the material.

REFERENCES

1. K. Nawa, N. Suda, Y. Fukao, T. Sato, Y. Aoyama, and K. Shibuya, Earth, Planets Space **50**, 3–8 (1998); K. Nawa, N. Suda, Y. Fukao, T. Sato, Y. Aoyama, and K. Shibuya, Earth, Planets Space **50**, 887–892 (1998).
2. T. Tanimoto, J. Um, K. Nishida, and N. Kobayashi, Geophys. Res. Lett. **25**, 1553–1556 (1998).
3. T. Tanimoto and J. Um, J. Geophys. Res., B **104**, 28723–28739 (1999).
4. K. Nishida, N. Kobayashi, and Y. Fukao, Science **287**, 2244–2246 (2000).
5. A. Rhie and B. Romanowicz, Nature **431**, 552–556 (2004).

6. K. Nishida and Y. Fukao, J. Geophys. Res. **112**, B06306 (2007).
7. E. M. Lin'kov, L. N. Petrova, D. D. Zuroshvili, Trans. USSR Acad. Sci. Earth Sci.: Sect. **306**, 13–16 (1991).
8. S. I. Ermolenko, G. M. Shved, Fundam. Prikl. Gidrofiz. **9** (4), 3–6 (2016).
9. G. M. Shved, S. I. Ermolenko, and P. Hoffmann, Izv., Atmos. Ocean. Phys. **51**, 498–504 (2015).
10. S. Rosat, J. Hinderer, and L. Rivera, Geophys. Res. Lett. **30**, 2111 (2003).
11. S. Rosat, T. Sato, Y. Imanishi, J. Hinderer, Y. Tamura, H. McQueen, and M. Ohashi, Geophys. Res. Lett. **32**, L13304 (2005).
12. G. Roult, J. Roch, and E. Clevede, Phys. Earth Planet. Inter. **179**, 45–59 (2010).
13. V. K. Milyukov, M. P. Vinogradov, A. P. Mironov, A. V. Myasnikov, and N. A. Perelygin, Izv., Phys. Solid Earth **51** (2), 176–190 (2015).
14. W. Zürn, G. Laske, R. Widmer-Schidring, and F. Gilbert, Geophys. J. Int. **143**, 113–118 (2000).
15. N. Florsch, J. Hinderer, D. J. Crossley, H. Legros, and B. Valette, Phys. Earth Planet. Inter. **68**, 85–96 (1991).

Translated by A. Kobkova